A&A 372, 95–104 (2001)
DOI: 10.1051/0004-6361:20010380

Astronomy & Astrophysics

The association surrounding NGC 2439*

N. Kaltcheva[1,3], R. Gredel[2], and C. Fabricius[3]

[1] Department of Astronomy, University of Sofia, 5 James Bourchier Avenue, 1164 Sofia, Bulgaria
[2] Max-Planck-Institut für Astronomie, Königstuhl 17, 69117 Heidelberg, Germany
e-mail: gredel@mpia-hd.mpg.de
[3] Niels Bohr Institute for Astronomy, Physics and Geophysics, Juliane Maries Vej 30, 2100 Copenhagen Ø, Denmark
e-mail: cf@astro.ku.dk

Received 9 October 2000 / Accepted 6 March 2001

Abstract. The structure of the field surrounding the Galactic cluster NGC 2439 is studied utilizing *uvbyβ* photometry of bright OB stars. We collate all photometric and kinematic data available to identify possible groupings. The stars of our sample show a large scatter in their distances, radial velocities, proper motions and reddenings. We conclude that they do not belong to a single stellar association. We find evidence of the existence of three coherent structures at distances of 370 pc, 1 kpc, and 2.6–3.2 kpc. The high stellar density toward NGC 2439 is very likely due to a decreased absorption in this direction, which poses some doubt on the reality of the cluster. A comprehensive *uvbyβ* study of NGC 2439 is required to clarify its nature. The spatial distribution of the stars and their reddening are used to characterise the spatial distribution of the visual extinction in the region. The results obtained confirm previously determined constraints on the formation mechanism of interstellar CH^+ towards the NGC 2439 field.

Key words. stars: early type – stars: fundamental parameters – open clusters and associations: individual: NGC 2439 – ISM: clouds

1. Introduction

The physical parameters inferred from photometry, such as reddening and distance, are fundamental in the study of interstellar molecular absorption lines towards OB supergiants. The visual extinction is often used to estimate the fractional abundances of the observed molecules, and the distance of the background star is used to estimate the location of the foreground material where the molecular absorption lines arise. In particular, the observation of stars in a given OB association which are presumably at similar distances allows to relate changes in the fractional molecular abundances to changes in the optical depth of the translucent cloud. This is an important constraint which is not relevant to a sample of arbitrarily distributed stars.

A particularly interesting case concerns the study of interstellar molecules towards stars surrounding the Galactic cluster NGC 2439 (Gredel 1997, 1999). Gredel (1997) observed six stars in the field and detected interstellar absorption lines of CH and CH^+ towards all of them. From the visual extinctions A_V compiled by Humphreys (1978), Gredel (1997) established a clear correlation of the CH^+ column density with A_V. All observed stars were assumed to be members of the presumed association surrounding NGC 2439. That assumption provided the main argument to favor formation sites of interstellar CH^+ closely associated with the cold molecular material, and to reject models which involve CH^+ formation in regions of low-density material.

The question whether or not the stars surrounding NGC 2439 are associated with the cluster is, however, highly controversial. The field of NGC 2439 shows a highly non-uniform reddening and is very rich in apparent, local clumps of OB stars. Previous discussions of the existence of coherent groupings of stars, and their relation to the cluster NGC 2439 and to the nebulous condensations, were mainly based on spectroscopic or *UBV* absolute magnitude calibrations. In a recent work, Kaltcheva & Hilditch (2000, KH00 hereafter) showed that *uvbyβ* photometry may significantly improve the accuracy of stellar distances

Send offprint requests to: Kaltcheva,
e-mail: nadia@phys.uni-sofia.bg

* Table 2 is only available in electronic form at the CDS via anonymous ftp to cdsarc.u-strasbg.fr (130.79.128.5) or via
http://cdsweb.u-strasbg.fr/cgi-bin/qcat?J/A+A/372/95

for this particular field. These facts prompted the study which we present below. In particular, we present $uvby\beta$ observations for a number of stars, and discuss all available photometric $uvby\beta$ and kinematic data.

The complete sample studied here is presented in Sect. 2. The section includes a comprehensive discussion of error sources and some apparent discrepancies for individual stars present in the literature. The structure of the stellar field towards NGC 2439 adopted in the past is discussed in Sect. 3.1. Our new results are given in Sect. 3.2. The section contains our new interpretation of stellar groupings in the NGC 2439 field. Accurate distances are presented and used, together with the reddening of the stars, to characterise the distribution of the interstellar material towards NGC 2439. Our findings support the main conclusions of Gredel (1997) concerning the formation of interstellar CH^+ in the NGC 2439 field.

2. The sample

2.1. Observations

We restrict our study to stars brighter than $V = 10$ mag and of spectral type earlier than B3. The main reason is the lack of data for the fainter stars and the later spectral types for this particular field. Our selection corresponds to the OB+ and OB0 luminous stars (LS), which are generally considered to be the best tracers of the spiral structure (Slettebak & Stock 1957) and of the ISM.

We obtained new photometric data for 11 stars in a region within 5° of NGC 2439. The stars were selected to complete as much as possible existing photometric $uvby\beta$ data in the field. The observations were performed during January 1998 and December 1998 with the Strömgren Automatic Telescope (SAT) of the Copenhagen University Observatory at La Silla, as a part of an ongoing program of $uvby\beta$ photometry in star-forming regions. The selection of standard stars, observing procedures and transformations to the standard systems for the two observing runs are described in detail in Kaltcheva & Olsen (1999, KO99 hereafter) and Kaltcheva et al. (1999). Our results are summarised in Table 1.

2.2. The complete sample

We have collated a complete magnitude limited sample of stars to investigate the structure of the field towards NGC 2439. To construct the sample, we collect all stars earlier than B3 and brighter than 10th mag from the HD, CPD, PPM or LS catalogues using Simbad. We include all stars listed by Humphreys (1978) as probable members of the NGC 2439 association even if some of the stars do not meet our selection criteria given above. The final sample of 56 stars is presented in Table 2 available in electronic form at the CDS via anonymous ftp to (`130.79.128.5`).

Complete Strömgren and Hβ data are available for 44 stars, from the compilation by Hauck & Mermilliod (1998, HM98 hereafter), from KO99, and from the present work. Two stars have $uvby$ data but no Hβ available. With our observations listed in Table 1, all stars considered by Humphreys (1978) as probable members to the NGC 2439 association have now complete Strömgren and Hβ data.

For 23 stars, V magnitudes are available both from HM98 and from the photometry obtained with the SAT (KO99 or this paper). The residuals obtained from the difference of the V magnitudes from HM98 and the SAT data (KO99 and present data) have a mean value of –0.014 (±0.020 standard error (sd hereafter)). The largest difference of –0.059 occurs for HD 62844 (LS 721, B3Iab). There are 4 stars with Hβ data available both from HM98 and SAT. The residuals have a mean value of –0.003(±0.021 sd). The values of the residuals are not significant since early B-type stars may show variability.

Comparisons of $uvby\beta$ data taken with the same equipment and standard stars utilized during the observations with the SAT to data from the individual sources used to gather the photometry for the field in the HM98 compilation, show a good agreement. This indicates that the collated photometric data are homogeneous, and systematic errors in the initial photometric data are not significant. In particular, there is a very good agreement between the data obtained with SAT during the January 1998 and December 1998 observing runs. An exception occurs for CPD–31 1785 where there is a difference for c_1. Most likely, the difference originates from a variability of the star. Alternatively, a larger error in the u pass band may explain the discrepancy.

Table 2 summarizes the information for all stars in our sample. The stars are ordered according to their HD numbers in the first column, or according to their CPD or LS number (second and third columns). The PPM number is given in the forth column for convenience. Column 5 identifies stars which have been linked in the past to a possible grouping (H: the association surrounding NGC 2439 (Humphreys 1978), b: the open cluster Bochum 15 (FitzGerald et al. 1976), N: NGC 2439 No 2, Cr: Collinder 140). The Galactic coordinates and MK classifications are given in Cols. 6–8. The $Vuvby\beta$ photometry adopted in our study and its source are listed in Cols. 9–14. The de-reddened photometry, the colour excesses E_{b-y} and V_0 are given in Cols. 15–19, respectively. The $\beta(c_0)$ values, whenever used in the M_V calculation (see the text below) are listed in Col. 20. The absolute magnitudes M_V, calculated distance r in parsecs and the radial velocity when available, are given in Cols. 21–23, respectively.

The Tycho-2 astrometric catalogue (Høg et al. 2000) was used to select visual double stars in the sample, for which the photometry may not be used to obtain physical parameters. We find that only for HD 57120 the photometry is not reliable for the calculation of M_V. For this star the *Hipparcos* distance is listed. For HD 59941 the Tycho-2 position is given. The position given in the Simbad data base appears to be incorrect.

The colour excesses in Table 2 are obtained via Crawford's (1978) calibration for LC V, IV and III and

Table 1. New photometric data of early B stars within 5° of NGC 2439 in the standard $uvby\beta$ system. The star identifications are given in the first column. The internal rms errors (m.e.) of one observation (weight 1) are listed after each photometric quantity. In Cols. 10, 11 and 15 the weight of V, the indices and β are listed, and Cols. 12 and 16 give the number of nights for each star observed in $uvby$ and in β.

Identification	V	*m.e.*	$b-y$	*m.e.*	m_1	*m.e.*	c_1	*m.e.*	VW	W	NN	β	*m.e.*	W	NN
Jan. 1998															
HD 57120AB	7.013	0.008	−0.083	0.003	0.105	0.004	0.159	0.008	5	5	4	2.647	0.007	1	1
HD 61687	6.786	0.005	−0.057	0.002	0.116	0.004	0.437	0.002	3	3	3	2.727	0.007	1	1
HD 62315	6.957	0.006	−0.076	0.005	0.112	0.004	0.274	0.011	2	2	2				
HD 66539	7.686	0.024	0.008	0.005	0.074	0.008	0.290	0.000	2	2	2				
HD 66582	7.350	0.001	−0.048	0.006	0.105	0.008	0.256	0.013	2	2	2				
CPD −28 2602	10.218	0.009	0.365	0.005	−0.045	0.007	0.117	0.008	1	1	1				
CPD −31 1785	8.915	0.008	0.228	0.005	−0.059	0.003	0.022	0.011	2	2	2				
Dec. 1998															
CPD −31 1785	8.907	0.004	0.212	0.005	−0.042	0.005	−0.008	0.005	2	2	2	2.583	0.009	2	2
CPD −32 1661	9.793	0.009	0.253	0.006	−0.056	0.003	−0.004	0.002	2	2	2	2.607	0.006	2	2
CPD −32 1689	10.142	0.025	0.340	0.001	−0.106	0.005	0.011	0.011	2	2	2	2.590	0.003	2	2
CPD −33 1682	9.848	0.005	0.416	0.005	−0.148	0.013	−0.043	0.014	3	3	2	2.612	0.009	2	2
CPD −33 1768	9.837	0.011	1.093	0.001	−0.362	0.004	0.366	0.013	2	2	2	2.552	0.009	2	2

from the calibration by Kilkenny & Whittet (1985) for LC II, Ib, Iab and Ia. We used $R = 3.2$ and $E_{B-V} = E_{b-y}/0.74$ to obtain V_0. The calibration by Balona & Shobbrook (1984) is utilized for all stars to derive the M_V values. The MK classifications are taken from the Simbad database, but for all stars the individual sources of the spectral classifications were checked. To evaluate existing discrepancies, we used a $[c_1]$∼$[m_1]$ diagram to compare the MK spectral types with the photometric classification. We find a very good agreement in general. Additionally, c_0 vs. β diagram was examined for possible luminosity class (LC) mis-classifications and for stars with Hβ emission. Again, the classifications were found to be consistent in general, with the exception of HD 63290, for which we adopt LC II, which is more consistent with the photometric classification, than the LC Iab adopted in Simbad. This puts HD 63290 about 200 pc closer to the Sun. For the three supergiants HD 61827, HD 62150 and HD 62844, we adopt classes Ib, Ia, and Iab, respectively. We evaluate effects on distances assuming the alternative LC classification of Iab, Iab and Ia, respectively, which is given in the literature. The difference in distance amounts to less than 10%.

The possible sources of errors in calculating the colour excesses and distances for the individual stars from the $uvby\beta$ calibrations are recently discussed in detail by KH00. We find a good agreement between the MK classification and the photometry for our sample, which indicates that the colour excesses obtained here are reliable. The presence of emission lines in the stellar spectra is the largest source of error in the calculated absolute magnitudes for early-type stars. In such cases, Hβ indices obtained from c_0 are generally used to calculate M_V (cf. Balona 1994). This is also recommended for Ia supergiants, for which the Hβ index is no longer a good luminosity indicator (cf. Crawford 1978; Moon 1985; Balona 1994; KH00). The same applies for Iab and Ib supergiants which are located above the reference line for the corresponding LC and may suffer from spectral emission. Expected uncertainties in M_V are of the order of ±0.3 for LC III-V and ±0.5 for supergiants (Balona & Shobbrook 1984). An uncertainty of ±0.3 mag in M_V propagates to an asymmetric uncertainty of –13 to +15% in the derived distance r, and uncertainties of ±0.5 mag result in –21 to +26% uncertainties in r. We estimate additional uncertainties of 3–5% which may arise from possible systematic differences in c_1 of the various data sets used here.

We compare the photometric parallaxes of the stars in the sample (obtained as the reciprocal of the distances listed in Table 2) to the *Hipparcos* parallaxes, when available. The difference between the *Hipparcos* and the photometric parallaxes as a function of the visual magnitude V is shown in Fig. 1. There is an overall agreement between the two sets of parallaxes. Four supergiants are involved in this comparison, all of which are close to the zero line. Only CPD −27 2143, the faintest star in this comparison subsample, shows a deviation between photometric and trigonometric parallax of more than two sigmas. The *Hipparcos* parallax of 3.59 ± 1.32 mas dominates the formal error in this case, but we cannot exclude imprecise spectral classification or peculiarity. The star is classified as B0.5IIIn by Garrison et al. (1977). The LC is in agreement with the photometric classification, but the β index may be influenced by emission. If we use $\beta(c_0)$ instead, the distance is reduced to 2212 pc, which still does not agree with the *Hipparcos* parallax.

3. Discussion

3.1. Previous work

NGC 2439 is known as a sparse open cluster located towards an apparent absorption hole in the large emission

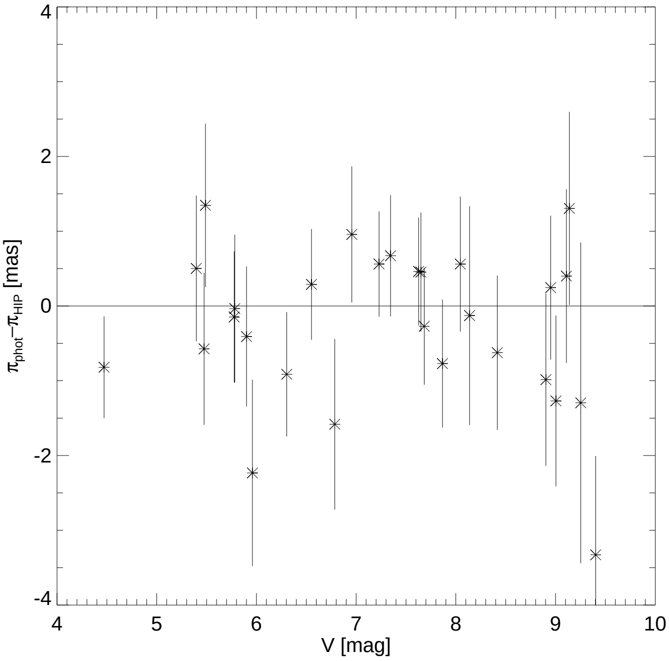

Fig. 1. The difference between the *Hipparcos* and photometric parallaxes plotted as a function of the visual magnitude V for stars in our sample. The error bars are σ errors in the *Hipparcos* parallaxes and 25% error in the photometric distances.

nebulosity in Vela-Puppis, with a mean visual extinction $A_{\rm V}$ of 1.3 mag (Abt et al. 1957). Eggen (1983) noticed that the reddening in this direction is quite non-uniform and suggested that the cluster can actually result from an absorption hole. The available photometric distance determinations for the cluster vary widely: Zug (1933): 1.9 kpc, Becker (1959): 1.6 kpc, Turner (1977): 3.4 kpc, White (1975), Ramsay & Pollacco (1992): 4.45 kpc. The latter authors suggested that the cluster is physical, and not an optical effect. A distance of 3–4 kpc puts the cluster considerably below the Galactic plane, supporting the impression that the Population I material is less concentrated to a thin disk in this direction (Vogt & Moffat 1975).

Schmidt-Kaler (1961) suggested that the cluster is part of a larger OB association, which contains a prominent group of four bright B-type supergiants (SGs): LS 640, 675, 719 and 721 (HD 61827, HD 62150, CPD –32 1734, HD 62844). The group is referred to as the four SGs group in the following. The group is located about half a degree East from the cluster and it has been later noticed independently by Garrison et al. (1977). Turner (1977) studied a field 5° in diameter around NGC 2439 and identified a possible association of about 20 luminous OB stars, which he placed at 3.4 kpc, in accordance with his estimate of the cluster distance. We note that Turner (1977) did not use a consistent M_V calibration. One may speculate that this may have caused the agreement of the distances of the four SGs group and the rest of the suggested members. Some of the stars considered by Turner (1977) are assigned by FitzGerald et al. (1976) to the open cluster Bochum 15 – a loose aggregate of 28 OB stars, located at 4.4 kpc from the Sun according to ZAMS fitting and spectroscopic parallaxes. Later, based on new photometric and spectroscopic observations, Jackson et al. (1977) identified two possible aggregates in this direction: Bochum 15a/b at 3 and 5.2 kpc, respectively. Turner (1977) considered Bochum 15a as a subgroup of the NGC 2439 association. Eggen (1980, 1981, 1983) stipulated that the mean reddening of the clusters has been incorrectly applied to the four SGs group. The group is more heavily reddened and located at a distance of 1.9 kpc. Humphreys (1978) listed 15 OB stars and two later type SGs (CD −30 5135: F2Iab, HD 63804: A1Ia) as members of the association, which she placed at 3.2 pc. She noticed that the radial velocities, when available, do not support a common distance of the cluster SGs (HD 62058 (G1Ia), CD −31 4916 (M2Iab), CPD −31 1785 (B1.5 Ib)) and the association's SGs (LS 640, 675, 719 and 721; the two late type SGs mentioned above do not have $v_{\rm r}$ measured). In a discussion of the distribution of the bright LS towards Canis Major – Puppis – Vela, KH00 showed that the four SGs group and the OB clump of LS 538, 514, 507, 534, 528 and 511, located North-West from the cluster at $l = 242.5°$, $b = -4.4°$, might be indeed at different distances of 1.03 and 3.2 kpc, respectively. Both groupings were suggested by Humphreys (1978) to be associated with NGC 2439 as well. During her search for faint OB stars in Puppis, Orsatti (1992) noticed a previously undetected dense, heavily reddened group of 33 faint OB+ and OB0 LS at $(l, b) = (249°, -4°)$, 2.5 deg South-West from the cluster. Little is known about that group.

3.2. Structure of the field around NGC 2439

We investigate the spatial structure of the field in order to reveal spatially coherent groups of stars. Figure 2 presents the location of the program stars plotted in Galactic coordinates and the diagrams Galactic longitude vs. Colour excess ($l°$ vs. E_{b-y}) and Galactic longitude vs. distance ($l°$ vs. r). Figures 3a–c show the colour magnitude (CM), M_V vs. $(b-y)_0$, and the variable-extinction diagram, respectively. Open symbols are used for the weakly reddened, nearby stars. We refer to them as foreground stars in the following, opposite to background stars at larger distances. We use symbols "*1*" and "*2*", as in KH00, to mark the four SGs group and the clump at $l = 242.5°$, $b = -4.4°$. For the stars in the immediate vicinity of NGC 2439 (HD 61851, 61709, CPD –31 1781) we use "+" symbols, and "N" for the star NGC 2439 No 2. The stars assigned to Bochum 15 are marked with "b". All other stars are marked with dots. The asterisk identifies LS 779, which is the star with the largest visual extinction ($A_{\rm V} = 5.18$ mag) in our sample. LS 640 and 675, which have been linked both to the four SGs group and to Bochum 15, are represented by "*1*".

Figure 2 demonstrates that the visual extinction $A_{\rm V}$ across the field is below 0.12 mag up to a distance of

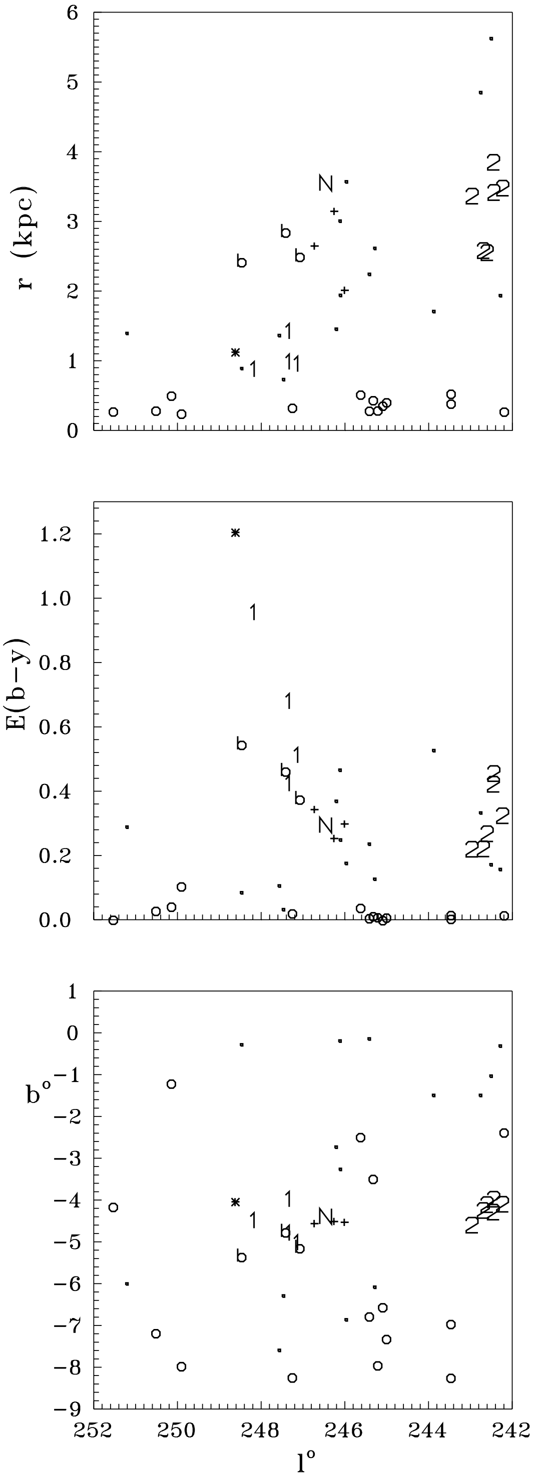

Fig. 2. The program stars plotted in Galactic coordinates and the diagrams Galactic longitude vs. colour excess and Galactic longitude vs. distance. Open symbols – foreground stars; *1*,*2* – four SGs group and the clump at $l = 242.5°$, $b = -4.4°$, respectively, "+" – the stars in the immediate vicinity of NGC 2439; "N" – NGC 2439 No 2; "b" – Bochum 15 stars, asterisk – LS 779.

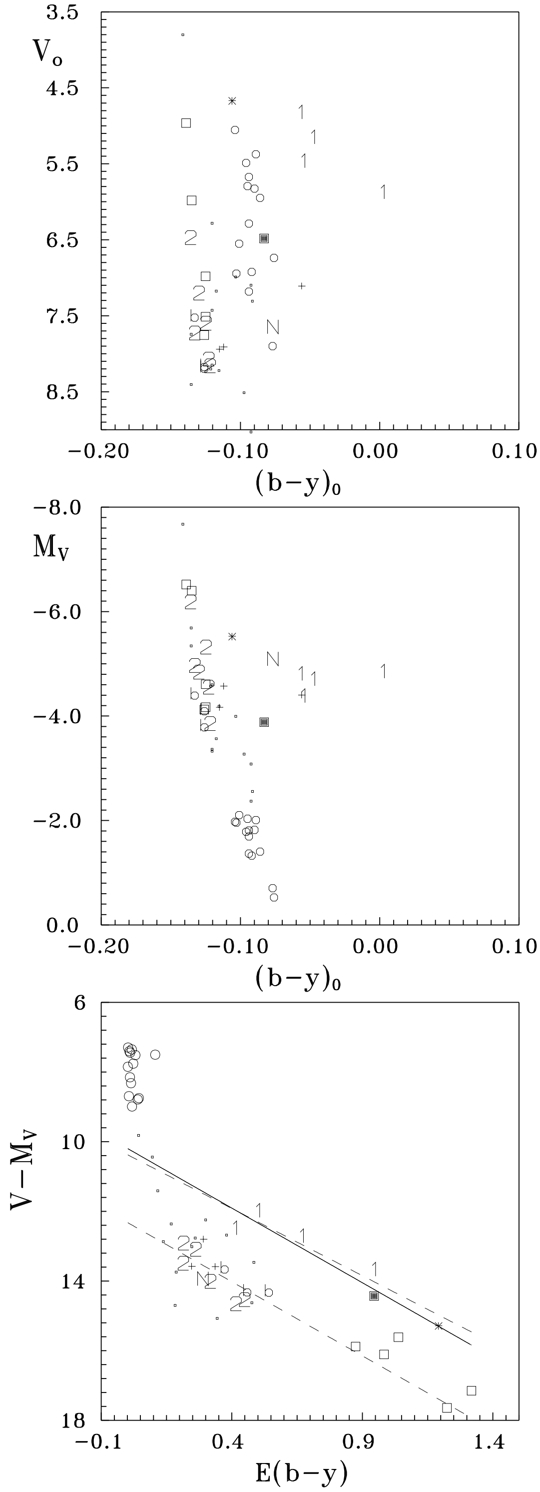

Fig. 3. The CM, M_V vs. $(b-y)_0$ and variable-extinction diagrams for the field. The solid line in the bottom plot presents the $R = 3.2$ least squared fitting for the four SGs group. The symbols are the same as in Fig. 2. To mark the faint LS (Table 4) square symbols are used (filled square for LS 810).

300 pc. Beyond that distance, the visual extinction increases to about 1.2 mag at a distance of about 2.5 kpc. Towards the region of highest absorption, at $l = 249°$, A_V reaches 5 mag at about 1 kpc. In order to establish more precisely the spatial structure of the dust cloud at $l = 249°$, we searched the literature for additional stars with $uvby\beta$ data available which are located in this

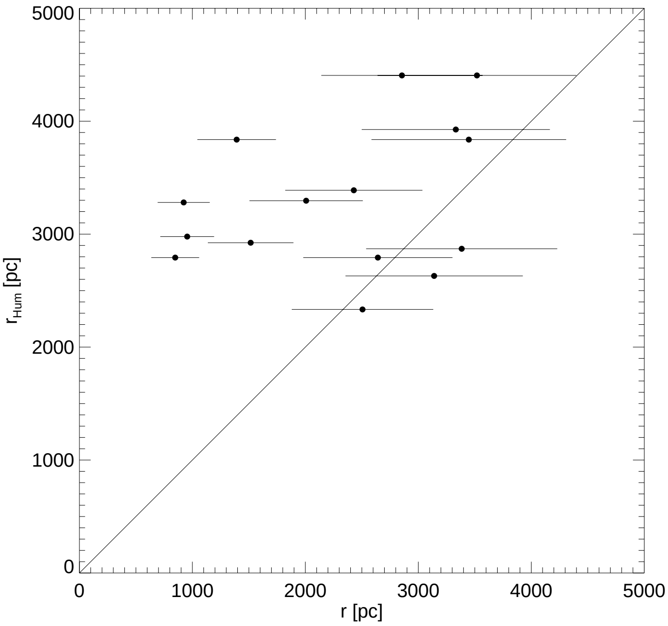

Fig. 4. The comparison of the distances obtained here to those adopted by Humphreys (1978). The error bars in the photometric distances correspond to 25% error.

Table 3. E_{b-y} and distances for 8 stars foreground to the dust cloud at $l = 249°$, $b = -4°$. The star identifications, MK classification and the Galactic coordinates are given in the first three columns.

HD	MK	$l°$	$b°$	E_{b-y}	r(pc)
61595	F8V	246.27	−04.86	0.000	60
62374	B5V	246.65	−04.19	0.109	624
62735	A9IV	246.79	−03.83	0.148	960
61989	F7V	247.94	−05.36	0.006	50
62539	F0IV	248.10	−04.84	0.010	72
63447	A9V	248.18	−03.78	0.015	199
63077A	G0V	249.13	−04.81	0.013	12
63639	F3V	249.21	−04.14	0.019	237

direction. Table 3 summarizes the results obtained for 8 stars. Colour excesses and distances are obtained from the calibrations by Crawford (1975, 1979). Towards $l = 246°$ the colour excess E_{b-y} rises linearly with distance until 960 pc, revealing an absorption hole in the direction of NGC 2439. Towards $l = 248°$–$249°$, only nearby stars with a distance closer than 250 pc are present. This implies that the $248° - 249°$ dust cloud is nearby and possibly located at a distance of about 200–250 pc.

We find an excellent agreement between our values of the colour excesses and those obtained by Humphreys (1978). However, large discrepancies exist in the derived distances. A comparison of our distances with those of Humphreys (1978) is given in Fig. 4. It appears that the distances adopted by Humphreys (1978) tend to be over-estimated. Possibly, the discrepancy arises from an over-estimation of the spectroscopic distances (see KH00 for a recent discussion). Our results show a large spatial spread of about 2.7 kpc for the stars in Humphreys' list. This makes it unlikely that all stars be part of a single OB association. Our photometric distances do indicate the presence of two spatial concentrations of the stars in Humphreys' (1978) list, at distances of about 1 kpc and of 3 kpc.

Our full data set clearly indicates the presence of three spatial structures towards the NGC 2439 field (cf. Figs. 2 and 3). Firstly, there are foreground stars located at an average distance of 370(±99 sd) pc. We identify a total of 14 foreground stars. All foreground stars are weakly reddened, with visual extinction $A_{\rm V} < 0.5$ mag and a mean value of 0.1 mag. The M_V vs. $(b-y)_0$ diagram indicates that these are all low-mass stars. The foreground stars located at $b = (-6°, -8°)$, $l = (244°, 246°)$ are possible members of the Cr 140 group. Secondly, the four SGs group is located at a distance of 1.03 kpc (see KH00 for a more detailed discussion). These stars are not uniformly reddened and $A_{\rm V}$ varies from 1.8 to 4.1 mag. The star LS 779 in the vicinity of the four SGs group is also located at a distance of 1 kpc. Thirdly, the bright stars closely surrounding NGC 2439 (identified with the "+" symbols), located at 2.6(±0.56 sd), and the group *2* located at 3.2(±0.50 sd) kpc, have a mean visual extinction $A_{\rm V} = 1.27$ mag. The possibility exists that group *2* is connected to the poorly investigated open cluster Haffner 11 at $(l, b) = (242.41°, -3.5°)$. The three stars of Bochum 15 (LS 628, 679, 681) which are included in our sample, are located at an average distance of 2.6(±0.23 sd) kpc and reddened by $A_{\rm V} = 2.0$ mag on the average. The star NGC 2439 No 2 is located at 3.5 kpc and is reddened by $A_{\rm V} = 1.24$ mag.

To better characterise the dense young group discovered by Orsatti (1992) towards the region of the largest visual extinction in the field, we searched the literature for $uvby\beta$ data of B-type stars located nearby. Table 4 contains the de-reddened photometry and derived quantities for 6 highly reddened relatively faint LS ($10.5 < V < 12$), based on $uvby\beta$ observations by Kilkenny (1993). These stars, marked with squares, are included in the diagrams in Fig. 3. The filled square identifies LS 810, which appears to be more evolved in comparison to the other stars given in Table 4. The stars show a large spread in distance, ranging from 1 to 3 kpc. The possibility exists that they form part of an extended young structure embedded in the cloud.

The variable-extinction plot in Fig. 3c (bottom panel) also reveals three distinct structures in the field. Apart from the foreground stars, the four SGs group is clearly separated from the more distant stars (denoted by b, +, N and *2* symbols) at 2.6–3.2 kpc. The dashed lines are linear least-square fittings for the latter two groups. The fitting parameters lead to distances 1.1 (±0.4 sd) for the four SGs group and 2.9 (±0.5 sd) for the (b, +, N and *2*) stars on the average. There is an agreement with normal ratios of total-to-selective absorption as well, and the star with the highest $A_{\rm V}$ value, LS 779, seems to obey it. Both LS 779 and LS 810 may be related to the four SGs group. We note that the variable-extinction method relies on the

Table 4. De-reddened photometry, E_{b-y}, M_V and distances for 6 faint LS located towards $l = 249°$, $b = -4°$.

LS	$(b-y)_0$	c_0	m_0	E_{b-y}	V_0	M_V	r (pc)
717	−0.135	−0.183	0.132	1.224	5.981	−6.399	2992
743	−0.125	−0.086	0.082	0.874	7.512	−4.609	2656
773	−0.139	−0.22	0.109	1.318	4.964	−6.518	1979
786	−0.126	−0.096	0.128	0.983	7.754	−4.124	2375
792	−0.125	−0.087	0.049	1.038	6.981	−4.169	1698
810	−0.083	0.346	0.158	0.945	6.483	−3.883	1184

determination of M_V and does not present an independent distance determination in comparison to that based on averaging the individual stars distances. The confidence in the distances calculated here is mainly based on the reliability of the Balona & Shobbrook (1984) M_V calibration (cf. Kaltcheva & Knude 1998), on the overall agreement with the *Hipparcos* data (Fig. 1), and on the photometric diagrams and the kinematic data.

By looking at the CM and $M_V/(b-y)_0$ diagrams, the stars of group *2* are very young and form a tight main sequence (MS). The same is true for the highly reddened, faint OB stars, which are located towards Orsatti's group, LS 810 being an exception. LS 640, 675, 719, 721 (i.e. the four SGs group), 779 and 810 are evolved stars (cf. our CM and M_V vs. $(b-y)_0$ diagrams). Possibly, they form an older structure which is located at a mean distance of 1.07(±0.3 s.e.) kpc. The stars of Bochum 15 and the rest of the faint LS listed in Table 4 are younger, more distant, and spread out in depth into the cloud. This may indicate an age gradient among the bright stars within the cloud, in the sense of a propagating star formation away from the Sun, but such a conclusion may be strongly biased because of the sparse data set. The bright stars towards NGC 2439 (including NGC 2439 No 2) have evolved away from the MS stars (cf. our CM and M_V vs. $(b-y)_0$ diagrams of Figs. 3a,b). The stars have very similar c_0 indices if compared with the four SGs group. This implies that they have similar luminosities. The stars are, however, some 2 magnitudes fainter than the four SGs group on the CM diagram. This finding supports the conclusion that distinct spatial structures among the background stars are present.

3.3. Kinematic considerations

The membership of stars to an OB association may also be based on the assumption of a common space motion of all members. The issue is, however, far from being trivial, as recently discussed by de Bruijne (1999). Figure 5a contains the vector point diagram $\mu_\alpha \cos\delta$, μ_δ for the program stars as obtained from the Tycho-2 (Høg et al. 2000) data, with their standard errors indicated. Only HD 63462 has no proper motion in Tycho-2 catalog and the *Hipparcos* proper motion is used instead. The foreground stars are marked with open circles and filled circles are used for the background stars. Figure 5b shows the proper

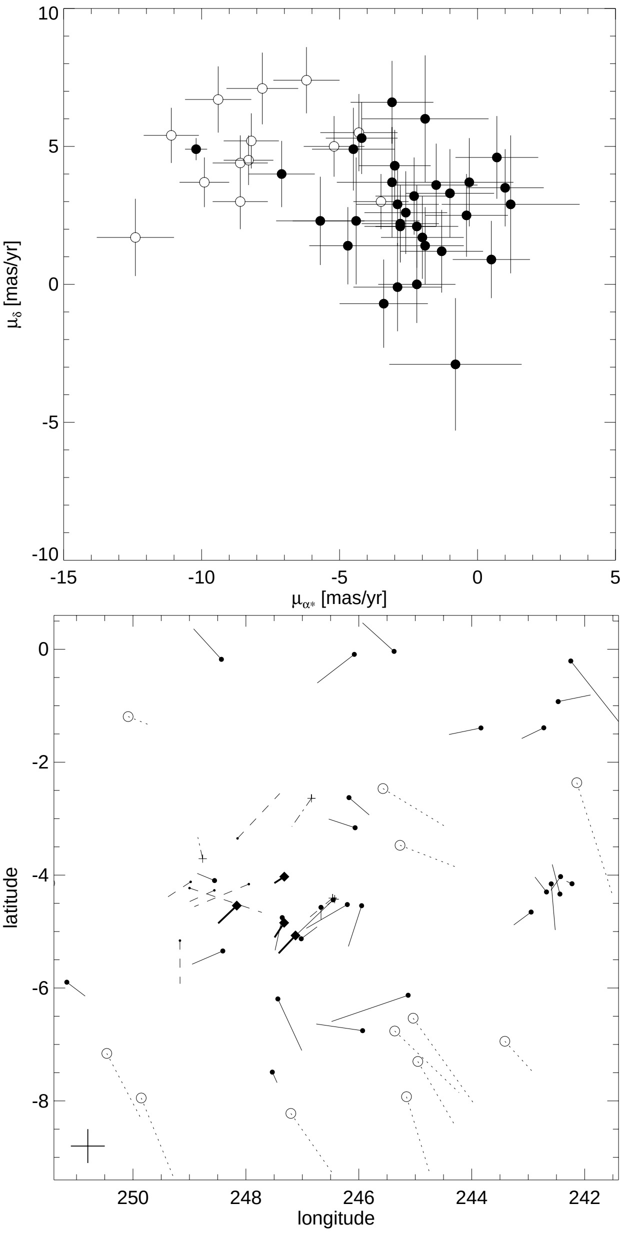

Fig. 5. a) Proper motions inferred from the Tycho-2 catalogue, with the standard errors indicated. Foreground stars are indicated with open circles. Filled circles are used for the rest of the stars. **b)** Proper motion vectors for all stars. The Galactic differential rotation has been subtracted for clarity. The cross in the lower left corner indicates the typical error bar of ±1.5 mas/yr of the Tycho-2 proper motions. Open symbols are used for the foreground stars, filled symbols for the rest of the stars from the sample. Solid diamonds are the four supergiants group, small filled symbols are the 6 faint LS, and "+" symbols are the 4 late type supergiants in the field.

motions obtained after subtraction of Galactic differential rotation using the Oort constants from Feast & Whitelock (1997). The stars from the four SGs group are marked with solid diamonds and vectors are represented by bold lines. Also shown are the four late type SGs in the field ("+" symbols) and the 6 highly reddened LS from Table 4 (dots). The cross in the lower left corner indicates the typical error bar of ±1.5 mas/yr of the Tycho-2 proper motions. From both plots the general difference between the foreground and background stars is evident, the background stars HD 63462 (−10.2, +4.9) being an exception. On the other side, coherent and well defined concentrations among the background stars are not evident, apart from the very similar motions of the four B-supergiants from group *1*. The proper motion of LS 779 agrees with that of group *1* within the errors, whereas that of LS 810 deviates. The two late type SGs assigned to the cluster, HD 62058 and CD −31 4916, exhibit the same proper motion as group *1*, but the radial velocity of HD 62058 (of $v_{\rm r} = +67.6$ km s^{-1}) is significantly larger than the mean radial velocity of group *1*.

OB associations may also be detected kinematically as their internal velocity dispersion is, in general, small. The available radial velocities support the existence of coherent groups at different distances. All foreground stars have radial velocities of $v_{\rm r} < 25$ km s^{-1}, with the exception of HD 62315. The four B-supergiants *1* are characterised by an average velocity of $v_{\rm r} = 44.42$ km s^{-1} with standard deviation of 7.09 km s^{-1}. The latter value is within the radial velocity dispersion limit for an OB association (Mathieu 1986). NGC 2439 No 2 and LS 528 (group *2*) have radial velocities of $v_{\rm r}$ above 70 km s^{-1}.

3.4. The translucent molecular cloud towards NGC 2439

The stars used by Gredel (1997, 1999) in his study of interstellar CH^+, CH, and C_2 in the NGC 2439 field are all included in the present work – the four SGs group, LS 779 and HD 63423. The new estimates of the colour excess, and especially of the distance allow us to study with greater confidence the correlation of the CH^+ column density with $A_{\rm V}$. The formation of interstellar CH^+ presents an outstanding problem in the field of interstellar chemistry (see Williams 1992 for a review). For this reason we re-evaluate the analysis and the main conclusions of Gredel (1997).

Figure 6a shows a plot of the CH^+ column densities $N(CH^+)$ as measured by Gredel (1997) versus the reddening E_{b-y} as obtained here. Figure 6b presents $N(CH^+)$ plotted versus r. The correlation of CH^+ column densities with reddening as established by Gredel (1997) is confirmed. In particular, the CH^+ column density increases with the optical depth of the molecular material as measured by the reddening E_{b-y} of the background star. On the other hand, $N(CH^+)$ does not depend on the distance r of the background star. This finding fully supports the conclusions of Gredel (1997) and rules out the possibility that increasing CH^+ column densities arise from increasingly large distances to the background stars. The data does suggest that the CH^+ column density is correlated with the optical depth through the foreground translucent molecular cloud. Processes which restrict the CH^+ formation sites to the surface of translucent clouds may thus be ruled out, unless a nesting structure of translucent clouds exists, where E_{b-y} is a measure of the number cloudlets along the line of sight.

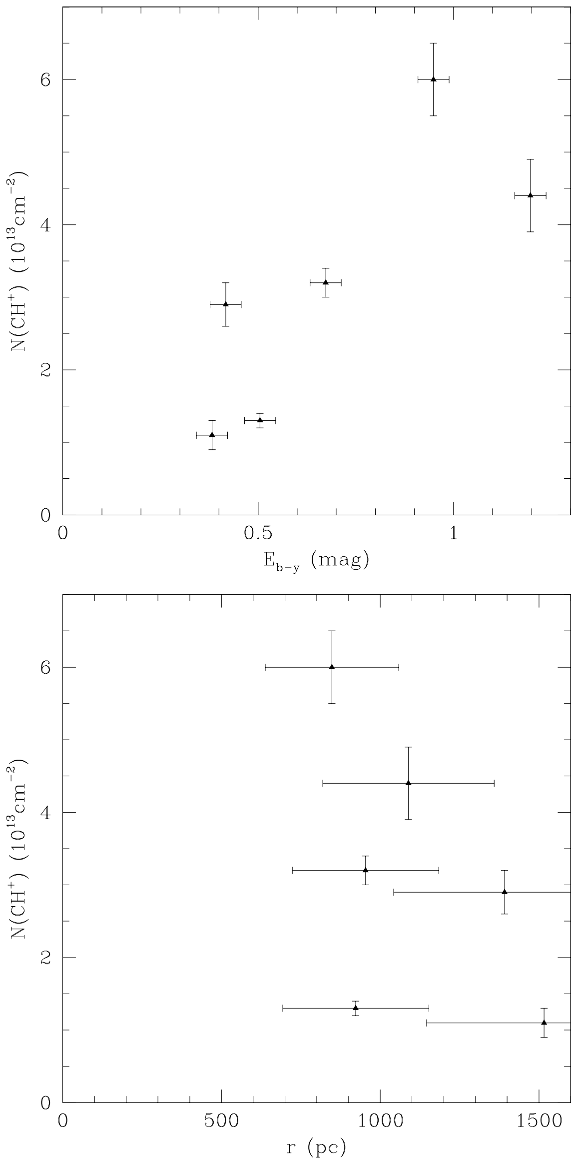

Fig. 6. a) CH^+ column densities $N(CH^+)$ versus the reddening E_{b-y}. The error bars in the colour excesses correspond to ±0.04 mag error. **b)** $N(CH^+)$ plotted versus r. The error bars in the photometric distances correspond to 25% error.

To further characterise the distribution of the visual extinction in the field, we compare the extinction derived from the $uvby\beta$ photometry with a star density map based on the USNO-A2.0 catalogue (Monet et al. 1998) in Fig. 7a. The stars are labeled with their extinctions, E_{b-y}, in units of 0.01 mag, on a background indicating the star density in the USNO-A2.0 catalogue. Stars brighter than blue magnitude (SERC-J) 18.5 were counted in $3' \times 3'$ pixels, with a dark colour indicating few stars counted. In order to derive $A_{\rm V}$, the extinction should be multiplied by 4.3. Figure 7b shows the *IRAS* 100 μm emission in the same field, with dark colour representing low emission. The squares mark the stars from our sample and the

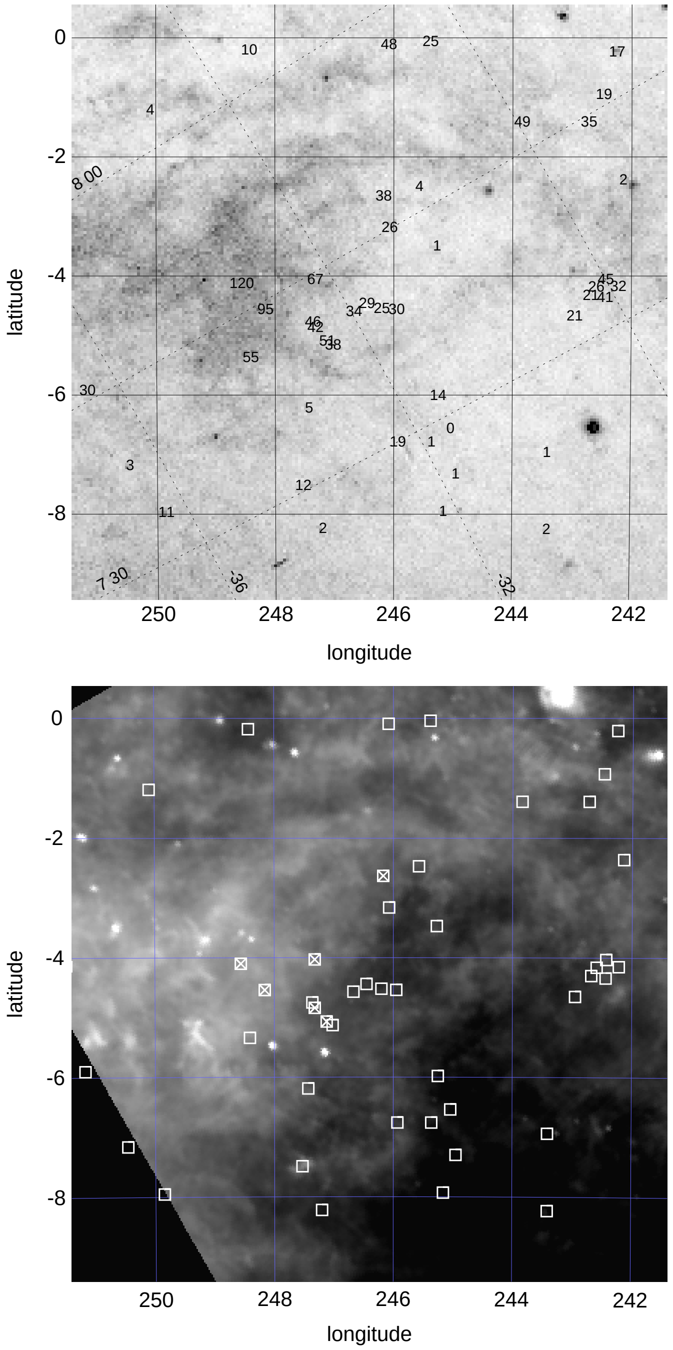

Fig. 7. a) The location of the program stars in Galactic coordinates, each star is labeled with its extinction, E_{b-y}, in units of 0.01 mag. The dotted lines indicate equatorial ICRS coordinates. The background indicates the star density in the USNO-A2.0 catalogue. As explained in the text, areas with few stars are the darkest. The round, dark spot is caused by a bright B5Ia star (HD 58350). **b)** The *IRAS* 100 μm emission map for the field. The program stars are marked with squares and the six stars used for the CH^+ observations are flagged with crosses.

six stars used for the CH^+ measurements are flagged with crosses. Both diagrams indicate the presence of a large absorbing cloud. It is immediately noted that the three stars with the largest reddenings are located towards the densest part of the cloud. This suggests that the cloud which is seen in Figs. 7a,b is situated either in the vicinity or in front of the stars. The variation of the colour excess across the field is not smooth. There is a general tendency of increasing foreground extinction with respect to Galactic latitude. East of the cluster, the visual extinction is highly non-uniform, and towards NGC 2439, an absorption hole becomes evident. This finding supports the conclusions of Sect. 3.2. The star count map of Fig. 7a shows an increased overall stellar density towards the cluster, apparently owing to a decreased absorption in this direction. The absorption hole is present both in the star count map and in the far IR emission map. Figure 7 raises considerable doubt whether the higher stellar density which appears towards NGC 2439 is real. It is clear that more $uvby\beta$ data for the cluster itself is needed to clarify whether or not NGC 2439 is a genuine Galactic cluster.

4. Concluding remarks

We have investigated the structure of the field towards the Galactic cluster NGC 2439 utilizing a complete magnitude limited sample of bright early type stars. We have collected all $uvby\beta$ photometric data and kinematic data which is presently available. The early type stars in the field show a large scatter in distance, radial velocities, proper motions and reddening. Our study emphasises the complexity of the region. We demonstrate that the stars in the field do not belong to a single OB association which is related to NGC 2439. We find evidence of a region of high absorption as close as 250 pc in the direction towards $l = 248°-250°$. The group of the B-supergiants LS 640, 675, 719 and 721 are spatially and kinematically related. Possibly, LS 779 (CPD –33 1768) and LS 810 belong to this group as well. The group appears to form a correlated structure at a distance of about 1 kpc and is located at $l = 247°-249°$. The group appears to be older than other stars in this direction. Its relation to Orsatti's stars is most interesting, and possibly indicates the presence of groups of different age which are embedded in the cloud. The cluster NGC 2439 is seen through an absorption hole with $A_V = 1.27$ mag. This finding poses some doubt on the reality of the cluster. At present, $uvby\beta$ data are available only for one star of NGC 2439, and a comprehensive study of the cluster is required to clarify the nature of NGC 2439.

The accurate distances and the reddenings of the stars obtained here support earlier conclusions that the CH^+ column density is correlated with the optical depth of the foreground translucent cloud. The finding rules out the possibility that towards NGC 2439, CH^+ forms along long pathlength of mainly diffuse interstellar material, or that it forms in intermittent dissipation bursts of interstellar turbulence. The correlation supports the suggestion of Gredel (1997) that the CH^+ formation sites are associated with the cold molecular material of the translucent cloud.

Acknowledgements. This work was supported by the Danish Space Board and NATO/Danish Research Council. This research has made use of the Simbad database, operated at CDS, Strasbourg, France.

References

Abt, H. A., Morgan, W. W., & Strömgren, B. 1957, ApJ, 126, 322
Balona, L. A. 1994, MNRAS, 268, 119
Balona, L. A., & Shobbrook, R. R. 1984, MNRAS, 211, 375
Becker, W. 1959, Zs. f. Ap., 48, 279
Crawford, D. L. 1975, AJ, 80, 955
Crawford, D. L. 1978, AJ, 83, 48
Crawford, D. L. 1979, AJ, 84, 1858
de Bruijne, J. H. J. 1999, MNRAS, 310, 585
Eggen, O. J. 1980, ApJ, 238, 919
Eggen, O. J. 1981, ApJ, 247, 507
Eggen, O. J. 1983, AJ, 88, 386
ESA 1997, The Hipparcos and Tycho Catalogues, ESA SP-1200, vols. 1–17
Feast, M. W., & Whitelock, P. A. 1997, MNRAS, 291, 683
FitzGerald, M. P., Hurkens, R., & Moffat, A. F. J. 1976, A&A, 46, 287
Garrison, R. F., Hiltner, W. A., & Schild, R. E. 1977, ApJS, 35, 111
Gredel, R. 1997, A&A, 320, 929
Gredel, R. 1999, A&A, 351, 657
Hauck, B., Mermilliod, M. 1998, A&AS, 129, 143 (HM98)
Høg, E., Fabricius, C., Makarov, V. V., et al. 2000, A&A, 355, L27
Humphreys, R. M. 1978, ApJS, 38, 309
Jackson, P. D., FitzGerald, M. P., & Moffat, A. F. J. 1977, A&A, 60, 417
Kaltcheva, N. T., & Hilditch, R. 2000, MNRAS, 312, 753 (KH00)
Kaltcheva, N. T., & Knude, J. 1998, A&A, 337, 178
Kaltcheva, N. T., & Olsen, E. H. 1999, A&A, 352, 600 (KO99)
Kaltcheva, N. T., Olsen, E. H., & Clausen, J. V. 1999, A&A, 352, 605
Kilkenny, D. 1993, SAAOC, 15, 53
Kilkenny, D., & Whittet, D. C. B. 1985, MNRAS, 216, 127
Mathieu, R. D. 1986, in Highlights Astron., 7, 481
Monet, D., Bird, A., Canzian, B., et al. 1998, USNO-A V2.0 A Catalog of Astrometric Standards, U.S. Naval Observatory
Moon, T. 1985, Communications of the University of London Observatory, No. 78
Orsatti, A. M. 1992, AJ, 104, 590
Ramsay, G., & Pollacco, D. L. 1992, A&AS, 94, 73
Schmidt-Kaler, Th. 1961, Zs. f. Ap., 53, 1
Slettebak, A., & Stock, J. 1957, Z. für A., 42, 67
Turner, D. G. 1977, AJ, 82, 805
Vogt, N., & Moffat, A. F. G. 1975, A&A, 39, 477
White, S. D. M. 1975, ApJ, 197, 67
Williams, D. A. 1992, Planet. Space Sci., 40, 1683
Zug, R. S. 1933, Lick Obs. Bull., 16, 132